# Relationship Between Cell Volume and Ion Transport in the Early Distal Tubule of the *Amphiuma* Kidney

WILLIAM B. GUGGINO, HANS OBERLEITHNER, and GERHARD GIEBISCH

From the Department of Physiology, The Johns Hopkins University School of Medicine, Baltimore, Maryland 21205; the Department of Physiology, The University of Wurzburg, Wurzburg, Federal Republic of Germany; and the Department of Physiology, Yale University School of Medicine, New Haven, Connecticut 06510

With appendices by L. MARIO AMZEL

From the Department of Biophysics, The Johns Hopkins School of Medicine, Baltimore, Maryland 21205

ABSTRACT The roles of apical and basolateral transport mechanisms in the regulation of cell volume and the hydraulic water permeabilities ($L_p$) of the individual cell membranes of the *Amphiuma* early distal tubule (diluting segment) were evaluated using video and optical techniques as well as conventional and Cl-sensitive microelectrodes. The $L_p$ of the apical cell membrane calculated per square centimeter of tubule is <3% that of the basolateral cell membrane. Calculated per square centimeter of membrane, the $L_p$ of the apical cell membrane is <40% that of the basolateral cell membrane. Thus, two factors are responsible for the asymmetry in the $L_p$ of the early distal tubule: an intrinsic difference in the $L_p$ per square centimeter of membrane area, and a difference in the surface areas of the apical and basolateral cell membranes. Early distal tubule cells do not regulate volume after a reduction in bath osmolality. Instead, they swell to an extent predicted from the change in osmolality. This cell swelling occurs without a change in the intracellular Cl content or the basolateral cell membrane potential. In contrast, reducing the osmolality of the basolateral solution in the presence of luminal furosemide diminishes the magnitude of the increase in cell volume to a value below that predicted from the change in osmolality. This osmotic swelling is associated with a reduction in the intracellular Cl content. Hence, early distal tubule cells can lose solute in response to osmotic swelling, but only after the apical Na/K/Cl transporter is blocked. Inhibition of basolateral Na/K ATPase with ouabain results in severe cell swelling. This swelling in response to ouabain can be inhibited by the prior application of furosemide, which suggests that the swelling is due to the continued entry of solutes, primarily through the apical cotransport pathway.

Address reprint requests to Dr. William Guggino, Dept. of Physiology, The Johns Hopkins University School of Medicine, 725 N. Wolfe St., Baltimore, MD 21205.

J. GEN. PHYSIOL. © The Rockefeller University Press · 0022-1295/85/07/0031/28$1.00 31

Volume 86 July 1985 31–58

## INTRODUCTION

The *Amphiuma* early distal tubule reabsorbs Na, K, and Cl preferentially to water and thereby dilutes tubule fluid. There is much evidence that a single apical cell membrane carrier that cotransports Na, K, and Cl plays a central role in the reabsorption of these three ions and is the site of action of the loop diuretic furosemide (Oberleithner et al., 1982*a*, *b*, 1983*a–c*). This nephron segment is also known to possess a Cl conductance on the basolateral cell membrane (Guggino et al., 1982; Oberleithner et al., 1983*d*), which allows the transcellular route for Cl—apical carrier-mediated entry and electrodiffusive exit—to be clearly defined. A similar model has also been proposed for the mammalian thick ascending limb (Greger, 1981; Greger and Schlatter, 1981).

These transport systems reabsorb solute in the absence of much water movement (Oberleithner et al., 1983*b*), thus making the *Amphiuma* early distal tubule a diluting segment as first described by Stoner (1977). Since the *Amphiuma* early distal tubule transports solutes preferentially to water, the epithelium must contain paracellular and transcellular barriers to water flow.

The volume of a renal epithelial cell, like the *Amphiuma* early distal cell, is determined by its intracellular solute content and extracellular osmolality, since at least one cell membrane or in some cases both cell membranes are quite permeable to water. Because transport processes are important in maintaining intracellular solute content, the same mechanisms may be responsible both for transepithelial solute transport and for regulating cell volume in response to changes in osmolality. For example, the basolateral Na/K ATPase is well known in renal epithelia to be a major factor in net transepithelial transport (see Katz, 1982, for a review). However, inhibition of Na/K ATPase with ouabain not only inhibits net solute transport but also results in significant cell swelling (Kleinzeller and Knotkova, 1964; Linshaw, 1980), which suggests that the basolateral pump also has a key role in cell volume regulation. In these systems, the cationic pump regulates cell volume, as suggested by Leaf (1956), by extruding $Na^+$, thereby offsetting the osmotic effects of nondiffusable macromolecules within the cell, and by maintaining solute gradients that can be used in volume control.

In contrast, it is also possible that in some circumstances, different transport systems may be involved in transepithelial transport and in regulating volume after changes in extracellular osmolality. For example, inhibition of the Na/K ATPase with ouabain in the frog urinary bladder does not cause significant cell swelling (Davis and Finn, 1981), which suggests that transport mechanisms separate from the Na/K pump can operate to control cell volume. It has been suggested that in the *Necturus* gallbladder (Ericson and Spring, 1982*a*, *b*), parallel Na/H and $Cl/HCO_3$ exchangers, located on the apical cell membrane, are involved primarily in cell volume regulation in response to osmotic shrinking, while an apical Na/Cl cotransporter is solely responsible for net transepithelial solute transport. Weinman and Reuss (1984), on the other hand, have observed that an apical Na/H exchanger may also play an important role in net solute transport across the gallbladder epithelium. Thus, it is still unclear how these different transport systems are regulated to coordinate simultaneously both cell volume regulation and transepithelial transport.

The aims of the present study are fivefold: (*a*) to develop a method for measuring the basolateral cell membrane potential and the cell volume simultaneously in the same cell; (*b*) to characterize the relative hydraulic water permeabilities of the apical and basolateral cell membranes; (*c*) to determine the response of early distal tubule cells to a hypo-osmotic stimulus; (*d*) to ascertain the role of basolateral Na/K ATPase in maintaining cell volume; and (*e*) to study the influence of the apical Na/K/Cl cotransport system in the response of early distal cells both to a hypo-osmotic stimulus and to the inhibition of basolateral Na/K ATPase.

## METHODS

### *Tubule Preparation*

Adult males and females of the salamander *Amphiuma means* were obtained from Carolina Biological Supply Co., Burlington, NC, and kept in tap water containing 10 meq/liter NaCl and 0.3 meq/liter KCl. After the animals were decapitated, their kidneys were

TABLE I

*Composition of Perfusion Solutions*

| | 1 | 2 | 3 | 4 | 5 |
|---|---|---|---|---|---|
| | *mM* | *mM* | *mM* | *mM* | *mM* |
| $Na^+$ | 96.3 | 71.3 | 71.3 | 21.3 | 21.3 |
| $K^+$ | 3.0 | 3.0 | 3.0 | 3.0 | 3.0 |
| $Ca^{++}$ | 1.8 | 1.8 | 1.8 | 1.8 | 1.8 |
| $Mg^{++}$ | 1.0 | 1.0 | 1.0 | 1.0 | 1.0 |
| $Cl^-$ | 83.6 | 58.6 | 58.6 | 8.6 | 8.6 |
| $HCO_3^-$ | 20.0 | 20.0 | 20.0 | 20.0 | 20.0 |
| $HPO_4^-$ | 0.56 | 0.56 | 0.56 | 0.56 | 0.56 |
| $H_2PO_4^-$ | 0.14 | 0.14 | 0.14 | 0.14 | 0.14 |
| Raffinose | 0 | 50 | 0 | 150 | 0 |
| Osmolality | 194 | 198 | 148 | 208 | 58 |

All solutions were bubbled with 98% $O_2$/2% $CO_2$. Bath solutions also contained 6 mM glucose and 3 mM glycine.

rapidly removed, cut into thin sections with a Stadie-Riggs tissue slicer (Arthur H. Thomas Co., Philadelphia, PA), and placed into continuously aerated Ringer solutions. Individual tubules were dissected using sharpened forceps and fine needles, and perfused according to the in vitro isolation-perfusion technique first described by Burg et al. (1966). Briefly, tubules were placed in a perfusion chamber and mounted on a concentric perfusion pipette system. On the perfusion side were an outer holding pipette and an inner perfusion pipette. The collection side had a holding pipette with Sylgard 182 (Dow Corning Corp., Midland, MI) for electrical isolation. The tubule chamber consisted of a trough cut in a Plexiglas plate. Since the chamber volume was ~0.5 ml and the perfusion rate was typically 10 ml/min, the entire contents of the bath exchanged in ~3 s. The composition of the perfusion solution is given in Table I.

In all experiments involving osmotic swelling, the cells were first bathed on both apical and basolateral sides with a solution in which the NaCl concentration was reduced and replaced with enough raffinose to match the osmolality of the control solution (solutions

2 and 4, Table I). The osmolality was then reduced by perfusing a solution with the identical ionic composition but without raffinose (solutions 3 and 5).

### *Electrical and Ion Activity Measurements*

The transepithelial potential difference ($V_{te}$) was measured at the tip of the perfusion pipette by means of a 3 M KCl–agar bridge–Ag/AgCl electrode located on the outlet port of the perfusion system and referenced to a 3 M KCl–agar bridge–Ag/AgCl electrode located in the outflow of the perfusion chamber. The location of the bridges in the outflow lines minimized any possible effects caused by KCl leakage from the bridges. $V_{te}$ was measured by an electrometer (KS-700, W-P Instruments Inc., New Haven, CT) and recorded on a stripchart recorder (model 2400, Gould Inc., Cleveland, OH). Measurements of the basolateral cell membrane potential difference ($V_{bl}$) were made with conventional microelectrodes, drawn on a microelectrode pipette puller (model PD-5, Narishige Scientific Instruments, Tokyo, Japan) from 1.2-mm-o.d., 0.5-mm-i.d., fiber-containing glass capillaries, and filled with 1 M KCl. Electrometer-microelectrode connections were made by Ag/AgCl wires. Electrodes were manipulated into position with a hydraulic micromanipulator (model MOR, Narishige Scientific Instruments) and cells were impaled by means of a sharp tap on the table.

The intracellular Cl activity ($A^i_{Cl}$) was measured with double-barreled microelectrodes, according to the techniques outlined by Fujimoto and Kubota (1976). The reference barrel contained 1 M Na-formate with 100 mM KCl, and the ion-sensitive barrel contained the new Corning Cl liquid ion exchanger (477913). The procedures for manufacturing these electrodes have been described in detail elsewhere (Oberleithner et al., 1982*a*). Cl electrodes were calibrated in pure solutions of 10, 50, and 100 mM NaCl. The average slope of the electrode response was 52.6 ± 2 mV/10-fold change in $A_{Cl}$. The selectivity of these electrodes to $HCO_3$ was similar to the values reported previously (Baumgarten, 1982). Because the contribution of $HCO_3$ to the Cl signal was only ~1 mV ($k_{Cl}$, $HCO_3$ = 0.12, $A_{HCO}$ = 15 mM), this error was neglected in our calculation of $A^i_{Cl}$. In contrast, the selectivity of Cl-sensitive microelectodes to furosemide was at least 15 times greater than that to Cl (see Oberleithner et al., 1982*a*). To avoid this problem, a concentration of furosemide was used ($5 \times 10^{-5}$ M) that was below the detectable limit of our electrodes.

To measure $A^i_{Cl}$, cells were impaled with double-barreled Cl electrodes according to the technique described above for conventional microelectrodes. The intracellular Cl activity was calculated from the following equation:

$$A^i_{Cl} = A^{bl}_{Cl} \times 10^{\left(\frac{V_{Cl} - V_{bl}}{S}\right)}, \quad (1)$$

where $A^i_{Cl}$ and $A^{bl}_{Cl}$ are the intracellular and basolateral Cl activities, respectively, $V_{Cl}$ is the potential difference sensed by the Cl electrode from the basolateral solution to the inside of the cell, $V_{bl}$ is the basolateral cell membrane potential difference, and $S$ is the slope of the electrode response. In all studies involving measurements of $A^i_{Cl}$, double-barreled electrodes were maintained within the same cell during a control period, followed by an experimental period and a return to control conditions.

### *Video-Optical Techniques*

A modified version of the video-optical system described by Spring and Hope (1979) and later by Davis and Finn (1981) was used to assess cell volume. The tubule was viewed through an inverted microscope (Diaphot-TMD, Nikon, Garden City, NJ) specifically modified to include differential interference optics (DIC). The light source was polarized by a polarizing filter placed in the condenser housing. The condenser lens was removed

and replaced by a revolving nosepiece containing a DIC prism (474571, Carl Zeiss, Inc., New York) in back of a 32× long-working-distance objective (E. Leitz, Inc., Rockleigh, NJ). The long-working-distance objective was important to allow access to the chamber by both perfusion and collection pipettes, while illuminating the tubule with a narrow beam of polarized light. The condenser was changed to a 10× lens by rotating the nosepiece when a large light beam was required to position the pipettes and perfuse the tubules.

The objective lens was either a Leitz 32× (0.40 numerical aperture [NA]) or a Zeiss 63× (1.25 NA) long-working-distance lens containing a second DIC prism (either 474571 or 434500, Carl Zeiss, Inc.) aligned in the same direction as the first. The image was analyzed by a second polarizer positioned until complete extinction of the polarized light was obtained. This optical system reduced the depth of field, making it possible to focus clearly at specific levels within the tubule.

The image was viewed by a television camera (model 66, Dage MTI, Michigan City, IN). Both the image signal and a time signal from a time signal generator (model TDG 200R, Pelco Sales Inc., Gardena, CA) were recorded on a videotape recorder (model 8950, Panasonic Matsushita Electric Industrial Co., Ltd., Secaucus, NJ) and displayed on a video monitor (model WV-5360, Panasonic Matsushita Communication Industrial Co., Ltd., Secaucus, NJ). The total magnification of the video-optical system with the 63× lens was ~3,500. With this magnification, only one cell was visible in the video monitor.

To assess the cell volume, the level of focus of the microscope was adjusted at approximately the center of the tubule lumen to give a side view of the cells along a portion of the tubule (see Figs. 1 and 2). Cells were chosen for recordings only if the midpoint of the cell was in focus and if both apical and basolateral surfaces could be seen clearly. In studies that involved measurements of $V_{bl}$ or $A^{i}_{Cl}$, the perfusion pipette was advanced through the lumen of the tubule to a position about one cell length away from the cell chosen for volume studies. A cell impalement was then made and the video image of the same cell was recorded. This allowed the determination of both volume and cell membrane potential to be made on an individual cell.

Images of cells recorded during the experiments were analyzed in the stop-frame mode by tracing the borders of cells onto plastic sheets without considering basolateral infoldings. The following parameters were measured: the outer tubular diameter ($R_o$), the minimum cell height ($h_o$) at the junction between cells (values measured at each junction were averaged), the maximum cell height ($h_m$) at the midpoint of the cell, and the cell length ($L$), which was taken as the distance between successive points at which $h_o$ was measured. In several instances, the cross-sectional area of the cell outlines was measured with a planimeter (model 620005, Keuffel & Esser Co., Morristown, NJ).

The cross-sectional area ($A_s$) of each cell outline was calculated as follows:

$$A_s = L(h_o/3 + 2h_m/3). \tag{2}$$

By considering one cell outline as representative of a section of the tubule, the volume ($V$) of an annulus of length $L$ was determined from the following equation:

$$V = \pi L[(R_o)^2 - (R_o - \langle h \rangle)^2], \tag{3}$$

where $\langle h \rangle$ is equal to $0.49h_m + 0.51h_o$. A detailed derivation of these equations is given in the Appendices.

In order to test the validity of our volume estimates, 10 optical sections, spaced 2 $\mu$m apart, were made with a 63× lens (depth of field 0.71 $\mu$m) on the side of the tubule. The sections overlapped the portion of a cell that was also used to determine the volume according to Eq. 3. This was accomplished manually by adjusting the fine-focus knob of

the microscope. Because this 20-$\mu$m section of the tubule represented only a portion of the volume of an annulus (see Fig. 9), the volume of a complete annulus was calculated according to the approach outlined in Appendix B. Hence, the magnitude of the volume calculated in this manner was comparable to that of Eq. 3.

The initial rate of change in cell volume ($k$) was calculated from a linear regression analysis of the volume measured at 5- or 10-s intervals for 30–40 s after a reduction of osmolality. The volume flux ($J_v$) was determined from the following equation, assuming the density of the bathing solution is 1:

$$J_v = (k)/A_t, \tag{4}$$

where $A_t$ is either the apical or basolateral surface area. $A_t$ was obtained by multiplying $2\pi R_o L$ by 1.5 for the apical cell membrane or 20.2 for the basolateral cell membrane. These factors were determined by Stanton et al. (1984) from a morphometric analysis of cell membrane areas in early distal tubules of *Amphiuma*. The hydraulic permeability ($L_p$) was calculated from:

$$L_p = \frac{J_v}{\Delta\pi}, \tag{5}$$

where $\Delta\pi$ is the difference in osmolality between control and experimental solutions. The validity of this calculation depends upon three assumptions: (*a*) that intracellular osmolality does not change considerably during the initial increase in cell volume; this is probably the case during the initial rate of increase in cell volume; (*b*) that unstirred layer effects are minimal; this assumption is discussed below; (*c*) that the reflection coefficient for raffinose is 1.

The osmotic permeability ($P_{osm}$) is described by the following expression:

$$P_{osm} = \frac{RTL_p}{V_w}, \tag{6}$$

where $R$ is the gas constant, $T$ is the temperature, and $V_w$ is the partial molar volume of water.

### *Statistics*

All data are given as means ± standard error (SE). The difference between means was assessed with Student's $t$ test. Paired or unpaired $t$ tests were used as necessary. $N$ is the number of cells, unless specified otherwise.

## RESULTS

### *Volume Measurements*

Figs. 1 and 2 are two views of a perfused tubule using differential interference optics. In both figures, the level of focus is approximately at the center of the lumen, with side views of cells visible on two sides of the tubule. Figs. 1 and 2 show side views of a tubule cell before (Fig. 1) and after (Fig. 2) a reduction in the osmolality of the basolateral solution. As expected, *Amphiuma* early distal tubule cells swell in response to a reduction of basolateral osmolality. These cells increase in volume by bulging into the tubule lumen without increasing in length or increasing the outer tubular diameter (specific values for these parameters are given in Tables IV, V, VI, and VIII).

The absence of a change in tubular length is important and has also been reported by Gonzalez et al. (1982) and Welling et al. (1983) following small changes in osmolality in studies on collapsed segments of mammalian proximal tubules. These studies and those of Gagnon et al. (1982), Linshaw (1980), and Linshaw and Stapleton (1978), in contrast to the present series of experiments, in which volume changes are expressed as increases in cell height into the tubule lumen, found that the cells of the mammalian proximal tubule swelled with a

FIGURE 1. This tubule was perfused in vitro with control lumen and bath solutions. The level of focus is at approximately the center of the lumen. The arrow points to a side view of a cell. Magnification ~1000.

significant increase in the outer diameter of the tubule. This discrepancy is clearly related to differences in the initial state of the tubules. In the mammalian studies, the lumen was collapsed and thus the cells could swell only by stretching the basement membrane. In our studies, the lumen was open and perfused, which made it possible for the cells to swell into the lumen.

Our technique for estimating volume, as discussed in the Methods, involves measuring the minimum cell height, the maximum cell height, the cell length, and the outer diameter of tubules from video images similar to the outlines shown in Figs. 1 and 2. The volume of an annulus of the tubule is then calculated

according to Eq. 3, assuming that the dimensions of the annulus are represented by those obtained from one cell image. To show that this technique gives a reliable estimate of volume that can be used in volume-related studies on individual cells, 10 optical sections of a portion of the tubule nearest to the coverslip were made. Each section was 2 $\mu$m from the other sections. The $A_s$ of each section was determined and the volume of the 20-$\mu$m portion of tubule was

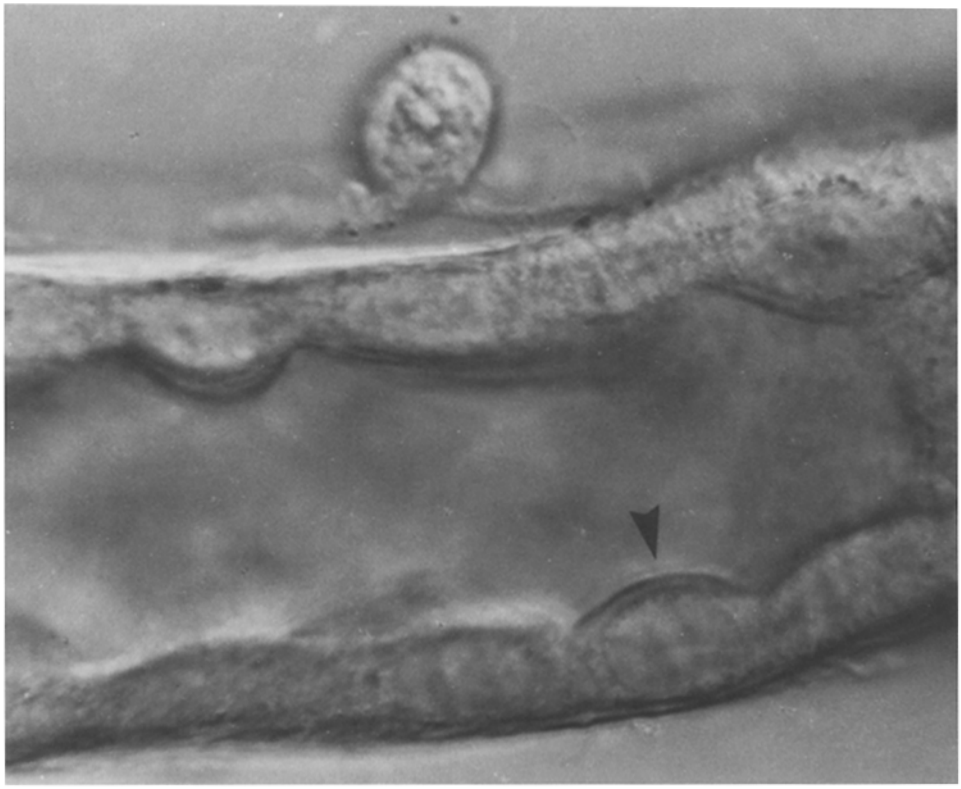

FIGURE 2. The same tubule illustrated in Fig. 1. However, in this experiment, the osmolality of the basolateral solution was reduced (solution 2 to 3). Note that the cells swell primarily by bulging into the lumen without significant changes in outer tubular diameter or cell length. The arrow points to the same cell shown in Fig. 1. Magnification ~1000.

calculated according to Eqs. B1 and B6 (see Appendix B). The data, given in Table II, are labeled Method B. In addition, at the midpoint of these cells, at a point that would have been chosen for the volume measurements presented in the rest of this manuscript, $V$ was determined according to Eq. 3. The results, given in Table II, are labeled Method A. A comparison of the data shows that there is no significant difference between the two techniques for measuring volume. This confirms that the equations given in the Appendices are valid and provide a reliable way of estimating tubular volume in our cells.

Furthermore, as an additional check of our techniques, $A_s$ was determined from 80 cell outlines both by measuring $h_o$, $h_m$, $L$, and the outside diameter, and by calculating $A_s$ from Eq. 2 and tracing the cell outline with a planimeter. The former method yielded an $A_s$ of 362 ± 14 $\mu m^2$; the latter gave an $A_s$ of 345 ± 13 $\mu m^2$. These values are taken from profiles of control as well as of swollen cells. Although there is a small but significant difference ($P < 0.001$) in these paired measurements, the difference is well within the variation in the cross-sectional area of the outlines, which again shows that our estimates reflect the true values reasonably well.

TABLE II

*Volume Estimates*

| | $V_m$ | $V$ | Percent change in $V$ |
|---|---|---|---|
| | $\mu m^3$ | $\mu m^3$ | |
| Method A | | | |
| Control | | 63,182±10,351 | — |
| Low osmolality | | 81,019±11,702 | 30±3 |
| Method B | | | |
| Control | 7,100±1,143 | 62,447±11,061 | — |
| Low osmolality | 10,224±1,323 | 80,143±11,503 | 33±7 |

In Method A, the volume was determined from only one optical section through the midpoint of a cell. In Method B, $V_m$, the measured volume, was determined from the cross-sectional area and the thickness (2 $\mu$m), according to Eq. B1, of 10 sections through the side of the tubule. Since each section was 2 $\mu$m from the other sections, a 20-$\mu$m portion of the tubule was optically sectioned as depicted in Fig. 9. $V$, the annulus volume, was calculated according to Eq. B6. The control solution was solution 2; low osmolality, perfused on the basolateral side only, was solution 3. $N$ = 6 cells, 6 tubules.

### *Apical and Basolateral Water Permeabilities*

A representative example of the initial rate of cell swelling after a reduction in basolateral osmolality in a control tubule is given in Fig. 3 (solid line). Reducing the osmolality of the basolateral solution causes this cell to swell at a rate that is linear for ~40–50 s. The maximum cell volume is attained in ~2–3 min. In all control cells analyzed, there was no tendency toward volume-regulatory decrease, with cells remaining at their maximum volume for at least 30 min after exposure to reduced osmolality. Thus, *Amphiuma* early distal tubule cells do not regulate volume under these circumstances and within this time period. However, it must be stressed that in some cells, volume regulation is a slow process that requires several hours to complete. For example, in *Amphiuma* red blood cells, volume regulation after cell swelling occurs over a period of 2 h (Cala, 1980). Thus, it is possible that early distal tubule cells do indeed regulate their volume but require a long period of time to do so. The average values of the initial rate of change in cell volume are given in Table III, as well as average values for $J_v$, $L_p$, and $P_{osm}$. These data indicate that the basolateral cell membrane is permeable to water.

In sharp contrast, identical 50-mosmol reductions of the osmolality of the apical solution had no significant effect on cell height or volume, which suggests that the water permeability of the apical cell membrane is low. Because of the low water permeability, the values for $k$, $J_v$, $L_p$, and $P_{osm}$ reported in Table III for the apical cell membrane were those obtained after a 150-mosmol reduction in the osmolality of the apical solution. Only under this condition were reproducible changes in cell volume observed.

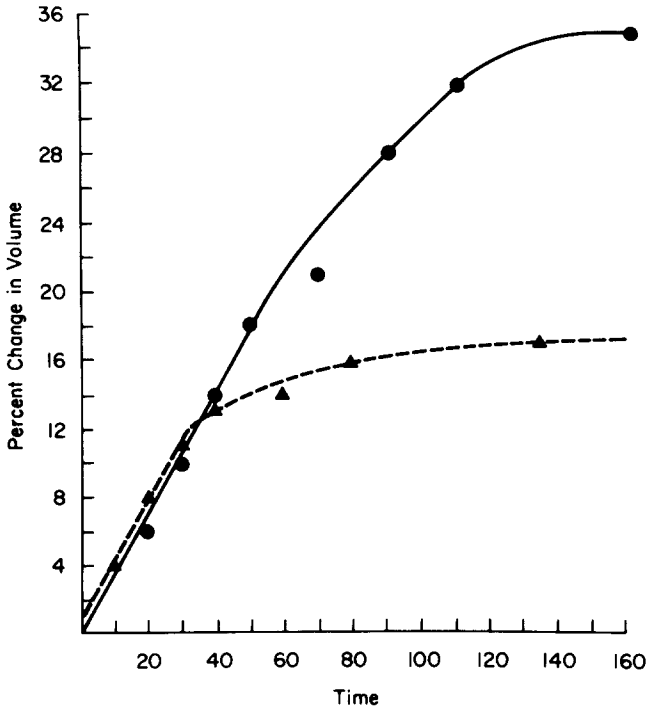


FIGURE 3. The percent change in cell volume (ordinate) following a reduction in the osmolality of the basolateral solution is plotted as a function of time (abscissa) for the same tubule first measured in the absence (solid line) and then in the presence (dotted line) of furosemide. The rate of increase in cell volume following the change in osmolality is linear for ~40–50 s. The plots do not go through the origin because of a small delay in the changing of the solutions. Because of possible uncertainties in the 0–10-s time period involved in changing the solution and mixing in the chamber, the data in Table III were calculated from the rate of change in cell volume between 10 and 40 s. Note that the cell swells less after furosemide treatment.

*Effects of Hypo-osmotic Solutions*

Steady state increases in cell height and volume after a decrease in the osmolality of the basolateral solution are given in Table IV. Given the simple relationship (see House, 1974)

$$\text{mosmol}_1 \times (V_1 - b) = \text{mosmol}_2 \times (V_2 - b), \quad (7)$$

TABLE III

*Osmotic Water Permeabilities*

| | $k$ | $S$ | $J_v$ | $L_p$ | $P_{osm}$ |
|---|---|---|---|---|---|
| | $\mu m^3/s$ | $\mu m^2$ | $L \cdot cm^{-2} \cdot s^{-1}$ | $cm \cdot s^{-1} \cdot osmol^{-1}$ | $\mu m \cdot s^{-1}$ |
| Basolateral* ($N$ = 27 cells, 11 tubules) | 307±38 | 129,989±4,853 | 23±2 × $10^{-11}$ | 4.6±0.5 × $10^{-6}$ | 2.5±0.3 |
| Apical‡ ($N$ = 8 cells, 7 tubules) | 31±5 | 11,481±1,819 | 26±7 × $10^{-11}$ | 1.8±0.5 × $10^{-6}$ | 1.0±0.3 |
| $P$ | <0.001 | <0.001 | <0.001 | <0.001 | <0.001 |

These data are based on the actual membrane area, which considers surface area amplifications. $k$ is the rate of cell swelling, $S$ is the cell membrane surface area of an annulus of the tubule including membrane amplications, $J_v$ is the volume flux, $L_p$ is the hydraulic water permeability, and $P_{osm}$ is the osmotic permeability.

* Data are from a 50-mosmol reduction in basolateral osmolality. The apical solution was solution 2.

‡ Data are from a 150-mosmol reduction in apical osmolality. The basolateral solution was solution 4.

where $b$ is the nonsolvent volume (although we have not measured the parameter in early distal cells, L. Reuss [personal communication] has measured a value of ~18% in the *Necturus* gallbladder), and knowing that $\text{mosmol}_1 = 203$ and $\text{mosmol}_2 = 153$, the change in volume of a perfect osmometer should be 26%. The change in volume reported in Table IV for control tubules is not significantly different from the value expected from the change in osmolality and provides additional evidence that *Amphiuma* early distal tubule cells do not regulate their volume within the time of our experiments in response to a reduction in basolateral osmolality.

In order to study the influence of solute transport across the apical cell membrane on the osmotic response, the cells were challenged with a hypo-osmotic solution in the presence of furosemide, a loop diuretic that is known to block Na/K/Cl in this segment (Oberleithner et al., 1982*a*). The application of furosemide to the luminal solution causes the cells to swell to a steady volume that is smaller than in control (Fig. 3, dotted line). As shown in Table V, increases

TABLE IV

*Steady State Percent Increases in Cell Height and Volume: Effects of Hypo-osmotic Solutions*

| | $h_o$ | $h_m$ | $A_s$ | $V$ | Percent change in $V$ |
|---|---|---|---|---|---|
| | $\mu m$ | $\mu m$ | $\mu m^2$ | $\mu m^3$ | |
| Control | 9.2±0.5 | 9.7±0.6 | 311±21 | 45,421±3,280 | — |
| Basolateral (low osmolality) | 10.1±0.7 | 16.0±0.7 | 466±34 | 58,193±4,609 | 29±3.7 |
| $P$ | <0.01 | <0.001 | <0.001 | <0.001 | <0.001 |

These values were recorded 3–10 min after an exposure of the basolateral cell membrane to the low osmolar solution. The control osmolar solution (solution 2) and the low osmolar solution (solution 3) differed only with respect to raffinose, which was not present in the low osmolar solution. The area refers to the cross-sectional area of cell outlines. The average length of these cells was 32 ± 1 $\mu$m, the control volume per length of tubule was 1,367 ± 88 $\mu m^3/\mu m$, and the outside diameter of the tubules was 53 ± 4 $\mu$m. $h_o$ and $h_m$ are the minimum and maximum cell heights; $A_s$ is the cross-sectional area of an optical section calculated according to Eq. 2; $V$ is the volume calculated according to Eq. 3. $N$ = 17 cells, 8 tubules.

in cell height and volume after furosemide treatment are significantly smaller than the increases noted in its absence. The increase in cell volume, in this case, is much smaller than predicted from the change in osmolality, which demonstrates that only when the apical Na/K/Cl cotransport system is blocked can these cells reduce intracellular solute content in response to swelling. It is also interesting that in the presence of furosemide (see Fig. 3), the cells do not attain a volume close to that expected for an osmometer and then gradually decline toward the lower steady volume. This is the response most often observed in cells that regulate their volume after a hypo-osmotic challenge (see Persson and Spring, 1982, for an example). One explanation for this phenomenon is that because of the relatively low water permeability, reducing bath osmolality in the presence of furosemide induces solute loss concomitant with the entry of water. The implications of these observations will be evaluated further in the Discussion.

TABLE V

*Steady State Increases in Cell Height and Volume: Effects of Furosemide and Hypo-osmotic Solutions*

| | $h_o$ | $h_m$ | $A_s$ | $V$ | Percent change in $V$ |
|---|---|---|---|---|---|
| | $\mu m$ | $\mu m$ | $\mu m^2$ | $\mu m^3$ | |
| Apical (furosemide), basolateral (control) | 12.3±0.4 | 13.4±0.7 | 456±23 | 67,808±4,210 | — |
| Apical (furosemide), basolateral (low osmolality) | 14.0±0.7 | 19.2±0.0 | 604±28 | 75,998±4,461 | 19±2 |
| $P$ | <0.001 | <0.001 | <0.001 | <0.001 | <0.001 |

These values were obtained in a manner similar to those reported in Table IV, except that in this case the luminal solution contained $5 \times 10^{-5}$ M furosemide. The average length of these cells was 36 ± 1 $\mu$m, the control volume per length of tubule was 1,937 $\mu m^3/\mu m$, and the outside diameter of the tubules was 62 ± 1 $\mu$m. $N$ = 9 cells, 5 tubules.

### *Effects of Furosemide*

To study the direct effects of blocking luminal Na/K/Cl cotransport on cell volume, furosemide was added to the luminal solution of control tubules and of those already exposed to reduced osmolalities. The application of furosemide to the apical cell membrane in control osmolality (solution 1 or 2) increases $V_{bl}$ from −62 ± 4 to −77 ± 6 mV ($N$ = 5 tubules), values similar to those observed previously (Oberleithner et al., 1982*a*) without a significant change in cell volume (Table VI).

Inhibiting Na/K/Cl cotransport with furosemide in cells already swollen by hypo-osmotic solutions also hyperpolarizes $V_{bl}$ from −63 ± 3 to −76 ± 6 mV ($N$ = 5 tubules). However, in low osmolality, furosemide treatment causes decreases in cell height and volume that are significantly greater than in control (Table VI). The rate of reduction in cell volume in this case is 184 $\mu m^3 \cdot s^{-1}$. This value is lower than the rate of swelling induced by reducing the bath osmolality.

### *Intracellular Cl Activity*

To determine the effects of reducing basolateral osmolality, the intracellular Cl activity and basolateral cell membrane potential ($V_{bl}$) were measured using

double-barreled, Cl-selective microelectrodes. An example of a recording with a Cl-sensitive microelectrode is shown in Fig. 4. Immediately after the microelectrode impalement, there was a slow decline in $V_{bl}$, followed by a repolarization to the original potential. Similarly, the voltage deflections across the basolateral cell membrane resulting from transepithelial current injection were large immediately after the impalement, diminished during the decline in $V_{bl}$, and increased again during the repolarization phase. Since the transepithelial voltage deflections were unchanged during an impalement, this pattern was probably

TABLE VI

*Steady State Decreases in Cell Height and Volume: Effects of Furosemide*

| | $h_o$ | $h_m$ | $A_s$ | $V$ | Percent change in $V$ |
|---|---|---|---|---|---|
| | $\mu m$ | $\mu m$ | $\mu m^2$ | $\mu m^3$ | |
| Apical (control), basolateral (control) | 12.9±1.4 | 15.9±2.2 | 462±32 | 66,816±5,460 | — |
| Apical (furosemide), basolateral (control) ($N$ = 4 cells, 4 tubules) | 12.9±1.4 | 14.0±0.8 | 408±28 | 65,025±6,243 | −3.0±1.7 |
| $P$ | NS | NS | NS | NS | NS |
| Apical (control), basolateral (low osmolality) | 12.5±1.1 | 16.2±0.8 | 461±33 | 60,325±5,439 | — |
| Apical (furosemide), basolateral (low osmolality) ($N$ = 5 cells, 2 tubules) | 11.0±0.6 | 14.1±0.8 | 408±28 | 56,031±5,261 | 8.2±0.6 |
| $P$ | NS | <0.001 | <0.001 | <0.001 | <0.001 |

These results are from paired studies of the effects of luminal application of furosemide on cell volume in control solutions and in hypo-osmotic solutions. The experiments showing the furosemide effect in control solutions are not paired with those in hypo-osmotic solutions. The average cell length in control osmolality was 25 ± 2 $\mu$m, the volume per unit length was 2,729 ± 280 $\mu m^2/\mu m$, and the outside diameter of the tubules was 76 ± 3 $\mu$m. The average cell length in hypo-osmotic solutions was 31 ± 2 $\mu$m, the average volume per length was 1,919 $\mu m^3/\mu m$, and the outside diameter was 59 ± 5 $\mu$m.

caused by an initial increase in the ratio of apical to basolateral resistances shortly after the impalement, followed by a gradual decrease in the resistance ratio back to the control value as the membrane sealed around the electrode. Because of this voltage response to a cell impalement, experiments were chosen for study only if, in the control steady state, both $V_{bl}$ and basolateral voltage deflections returned to nearly their original peak values. The average control $A^i_{Cl}$ and $V_{bl}$ values, 12.5 ± 1.8 mM and −62 ± 4 mV, are not significantly different from those previously recorded from *Amphiuma* early distal tubule cells in the doubly perfused kidney (Oberleithner et al., 1982*a*).

Reducing the osmolality of the basolateral solution by 50 mosmol in a manner identical to the experiments in Tables IV and V caused a decrease in intracellular Cl activity without a change in the basolateral cell membrane potential (Fig. 5 and Table VII). Similarly, reducing the basolateral osmolality after luminal application of furosemide also caused a reduction in intracellular Cl activity

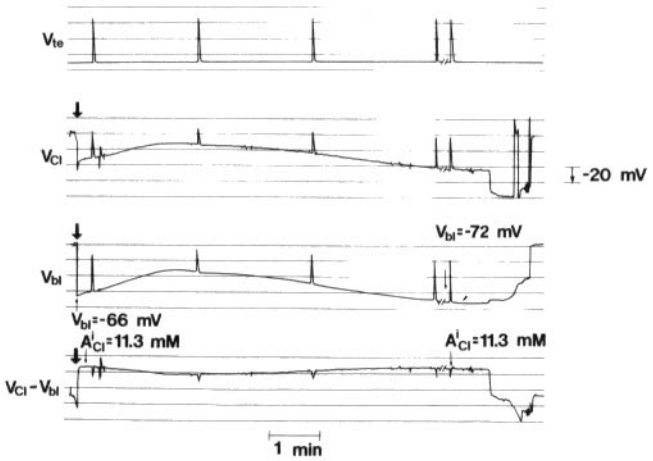


FIGURE 4. Four simultaneous voltage recordings. From top to bottom: the transepithelial potential difference ($V_{te}$), the potential difference measured by the Cl-sensitive barrel of a double-barreled microelectrode across the basolateral cell membrane ($V_{Cl}$), the potential difference measured by the reference electrode ($V_{bl}$), and the difference $V_{Cl} - V_{bl}$, which is directly proportional to intracellular Cl activity. The vertical deflections are the electrotonic voltage deflections resulting from the injection of $2 \times 10^{-7}$ A of current into the lumen. The arrows mark the point at which the electrode was impaled into a cell across the basolateral cell membrane. Note that the electrotonic voltages recorded by the reference electrode ($V_{bl}$) diminish shortly after the impalement and return to nearly their initial value as the cell recovers from the impalement. Representative values for $V_{bl}$ and calculated values of $A^i_{Cl}$ are included.

without a change in the basolateral cell membrane potential (Table VII). This is not significantly different from the change in intracellular Cl activity reported in the absence of furosemide.

The major difference between the two maneuvers is that, without furosemide, the decrease in intracellular Cl activity is not significantly different from the value calculated from the change in volume, whereas the fall in intracellular Cl

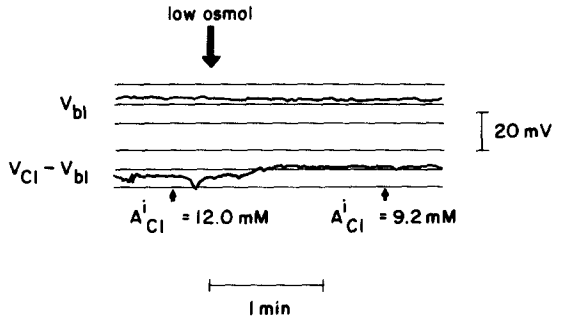


FIGURE 5. Recordings of the basolateral cell membrane potential, $V_{bl}$, and the difference $V_{Cl} - V_{bl}$. Reducing the osmolality of the basolateral solution reduces intracellular Cl activity without an effect on $V_{bl}$.

activity in furosemide-treated cells is significantly greater than the value predicted from a simple change in cell volume (see Table VII). This indicates that the swelling response is associated with a reduction in intracellular Cl content only in furosemide-treated cells, which is consistent with the observation that furosemide-treated cells swell less than predicted from the change in osmolality. Thus, early distal tubule cells can lose solute (probably K and Cl) during swelling but only after solute entry is inhibited by blocking the apical Na/K/Cl cotransport system with furosemide.

*Effects of Ouabain*

Early distal tubule cells of *Amphiuma* swell irreversibly in response to basolateral ouabain application. A sample time course of the change in volume is shown in Fig. 6. After a 2–3-min lag period, the cells swell, rapidly reaching maximum

TABLE VII

*Response of Steady State Intracellular Cl Activity to a Reduction in Basolateral Osmolality*

| Percent change in intracellular Cl activity | Measured | Predicted |
|---|---|---|
| Apical (control) | −26±5 | −22±1 |
| Basolateral (low osmolality) | | |
| Apical (control + furosemide) | −25±3 | −16±1 |
| Basolateral (low osmolality) | | |
| *P* | NS | <0.001 |

Measured values are those that were determined with ion-sensitive microelectrodes. The predicted values were calculated from all experiments reported in Tables IV ($N$ = 17 cells, 8 tubules) and V ($N$ = 9 cells, 5 tubules), according to the equation percent change in $A^i_{Cl} = V_1/V_2 - 1$, where $V_1$ is the initial value and $V_2$ is the final volume. Consequently, the predicted value is the change in $A^i_{Cl}$ expected solely from an increase in water activity without a change in Cl content.

cell volume after a 15–20-min exposure. The average rate of change is ~44 ± 6 $\mu m^3 \cdot s^{-1}$, which is ~85% slower than the rate of swelling induced by changing the bathing solution from isotonic to hypotonic. The magnitude of the change in cell height and volume after a 10-min exposure to ouabain is given in Table VIII. So drastic is the response to ouabain that, after 10 min, the cells often occlude the lumen.

Fig. 7 shows an example of the response of $V_{bl}$ to basolateral ouabain application measured in the same cell used for Fig. 6. Beginning ~1 min after ouabain application, $V_{bl}$ declines rapidly. Importantly, $V_{bl}$ responds more quickly than does cell volume to ouabain addition. For example, Fig. 7 shows that after a 3-min exposure to ouabain, $V_{bl}$ is reduced by ~20 mV, while, as illustrated in Fig. 6, there is still no detectable change in cell volume. These data may indicate that ouabain application causes a significant ion rearrangement or changes in ion conductance within the early distal tubule cell before affecting cell volume, but more studies are needed to prove this point conclusively. After a 10-min exposure to ouabain, both the average $V_{te}$ and $V_{bl}$ decline from +10 ± 3 and −66 ± 3 mV, respectively, in control, and to +2 ± 1 and −29 ± 1 mV after ouabain ($N$ = 7).

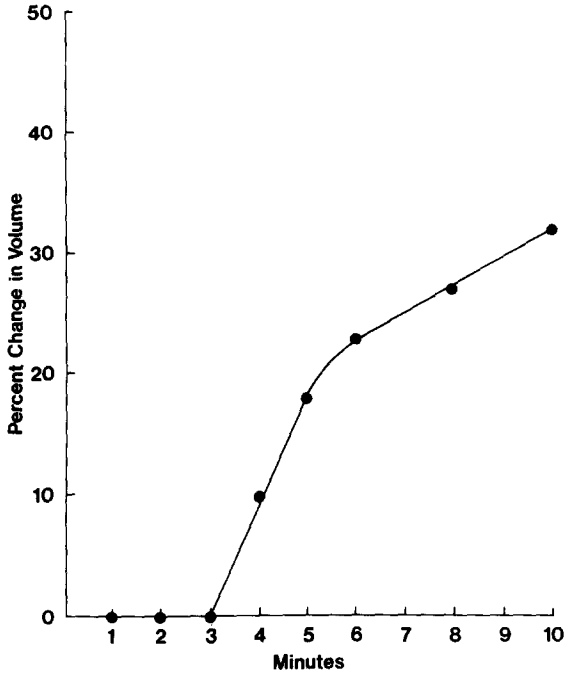


FIGURE 6. The percent change in cell volume (ordinate) after basolateral application of ouabain in minutes (abscissa) is shown. There is a 3-min lag period in this experiment between the basolateral application of ouabain and the beginning of cell swelling. This lag period is not caused by a delay in the solution change since this occurs within the first 5 s.

These relatively large effects of ouabain on cell volume and on the electrical potential differences can be significantly reduced by prior application of furosemide to the luminal solution. As indicated in Table IX, basolateral ouabain application for 10 min in the presence of luminal furosemide has no significant effect on cell height or volume. Similarly, as shown in Fig. 7, this same maneuver also inhibits the ouabain-induced decline in $V_{bl}$. In this condition, if ouabain is

TABLE VIII

*Steady State Percent Increases in Cell Height and Volume: Effects of Ouabain*

| | $h_o$ | $h_m$ | $A_s$ | $V$ | Percent change in $V$ |
|---|---|---|---|---|---|
| | $\mu m$ | $\mu m$ | $\mu m^2$ | $\mu m^3$ | |
| Control | 11.7±0.8 | 11.8±1.0 | 369±43 | 56,341±5,215 | — |
| Basolateral (ouabain) | 15.3±1.4 | 19.8±1.4 | 582±65 | 73,208±7,007 | 30±3 |
| $P$ | <0.005 | <0.001 | <0.001 | <0.001 | <0.001 |

These values were recorded 9–12 min after ouabain treatment. The average length of these cells was 30.5 ± 2.8 $\mu$m, the control volume per centimeter length of tubule was 1,893 ± 125 $\mu m^3/\mu m$, and the average outside diameter of the tubules was 61 ± 2 $\mu$m. $N$ = 11 cells, 5 tubules.

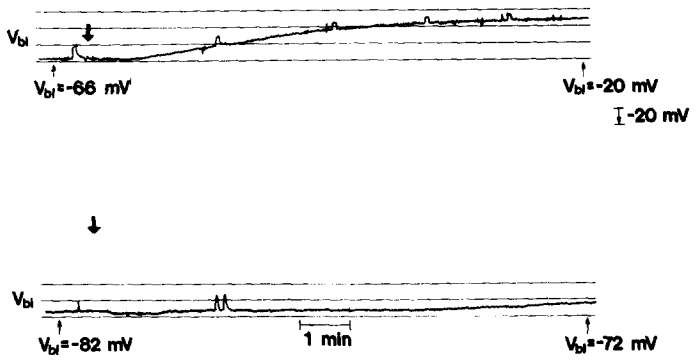


FIGURE 7. Two recordings of $V_{bl}$ using single-barreled conventional microelectrodes. The arrows mark the time at which ouabain was applied to the basolateral cell membranes. The upper trace shows the effect of ouabain measured in the same cell as in Fig. 6. After a delay of ~1 min, $V_{bl}$ declines rapidly, reaching −20 mV in ~10 min. Prior application of $5 \times 10^{-5}$ M furosemide to the apical cell membrane in a different cell delays the onset of the decline to ~9 min (lower tracing). After 10 min, $V_{bl}$ is still −72 mV. This small decline could be the result of other transport systems involving ion entry or could be caused by the lack of a complete block of apical Na/K/Cl cotransport by furosemide.

removed from the bath and then furosemide is removed from the luminal solution, the cells will remain viable, as evidenced by the continued maintenance of normal cell volume and cell potential. From these observations, it is safe to conclude that solute entry through the apical Na/K/Cl cotransport system is responsible for the time course of cell swelling shown in Fig. 6. We conclude, further, that because furosemide effectively inhibits ouabain-induced cell swelling, the apical Na/K/Cl cotransport system is the primary mechanism for solute entry into these cells.

TABLE IX

*Steady State Percent Increases in Cell Height and Volume: Effects of Furosemide and Ouabain*

| | $h_o$ | $h_m$ | $A_s$ | $V$ | Percent change in $V$ |
|---|---|---|---|---|---|
| | $\mu m$ | $\mu m$ | $\mu m^2$ | $\mu m^3$ | |
| Apical (furosemide), basolateral (control) | 11.8±0.4 | 11.6±0.8 | 353±27 | 51,013±4,534 | — |
| Apical (furosemide), basolateral (ouabain) | 12.2±0.4 | 12.2±0.6 | 390±35 | 53,875±5,009 | 6±1 |
| *P* | NS | <0.01 | <0.005 | <0.005 | <0.005 |

These values were recorded in a manner similar to those of Table VIII, except that the luminal solution contained $5 \times 10^{-5}$ M furosemide for several minutes before ouabain treatment. The average length of these cells was 32 ± 2 $\mu$m, the control volume per centimeter length of tubule was 1,588 ± 77 $\mu m^3/\mu m$, and the outside diameter of the tubules was 60 ± 2 $\mu$m. $N$ = 14 cells, 5 tubules.

## DISCUSSION

### *Volume Measurements*

The cell volume of the early distal tubule of *Amphiuma* was measured with video-optical techniques similar to those used by Spring and Hope (1979), Davis and Finn (1981), and Kirk et al. (1984). We have extended their techniques to experiments on *Amphiuma* renal cells and we show that estimates of both cell volume intracellular ion activities and basolateral cell membrane potentials can be obtained simultaneously in isolated and perfused renal tubules.

Before discussing the results, it is advantageous to examine a few of the methods that have been used to measure cell volume and compare them with the techniques reported in the present study. Spring and Hope (1979) and Davis and Finn (1981) have optically sectioned cells of sheet epithelia from apical to basolateral borders and have determined cell volume from the surface area of each section, the distance between the sections, and the number of sections. We have also optically sectioned a few tubule cells to validate the model described in the Appendices, and have calculated tubular volume. Instead of cross-sections, longitudinal sections (side views) of cells were taken on either side of a cell whose midpoint was in focus when the microscope was focused approximately at the midpoint of the tubule lumen (see Figs. 1 and 2).

Longitudinal sections were chosen for two reasons. First, despite the excellent views of the tubule cells provided by these optical techniques, we were unable to define clearly the exact border of each cell because of the complicated nature of the lateral interdigitations and basal infoldings of these cells (Stanton et al., 1984; Welling and Welling, 1978). Second, the diluting segment cells swell by bulging into the lumen. This means that a large central portion of the luminal surface of the cell extends into the lumen beyond the level of the tight junction ($h_m > h_o$). Thus, in sectioning from basal to apical surface, a point is reached where the outline of the lateral junction disappears, which makes it very difficult to determine the exact outline of the luminal membrane and the volume of the dome.

The majority of volume estimates in this study are made from a single longitudinal section (side view) of one cell, with the dimensions of this cell being used to calculate the volume of an annulus of the tubule of one cell length (see the Appendices). In a similar fashion, Kirk et al. (1984) have also used the dimensions of a single longitudinal optical section near the midpoint of the lumen to estimate the cell volume. They estimated cell volume by determining from a tracing of the tubule, ~100 $\mu$m in length, both the whole surface area and the surface area of the lumen. Dividing each area by the length gives the mean outside and inside diameters and allows calculation of volume from the equation $V_T$ (volume per tubule length) = $[(D_o)^2 - (D_i)^2]/4$. Hence, the tubule is modeled as if it were two cylinders, one inside the other.

### *Hydraulic Permeabilities of Apical and Basolateral Cell Membranes*

Our observations show that the water permeability of the apical cell membrane is much smaller than the water permeability of the basolateral cell membrane

and is thus a major barrier to transepithelial water flow. This appears to be a common phenomenon in epithelia in which solute transport is associated with relatively small water flow. For example, MacRobbie and Ussing (1961) observed that the osmotic water permeability of the apical cell membrane of the frog skin is at least 20 times smaller than that of the basolateral cell membrane. Similarly, Ganote et al. (1968) showed that cortical collecting duct cells swell only in response to a reduction in basolateral but not apical osmolality, which again suggests that the apical cell membrane water permeability is quite low. Thus, in both tissues, the apical cell membrane is a major barrier to water flow.

An asymmetry in the osmotic water permeability of certain epithelia in general, or of the early distal tubule in particular, may be a consequence of intrinsic differences in the properties of the individual cell membranes or, alternatively, the asymmetry may only be a result of differences between apical and basolateral surface areas. In the latter situation, the intrinsic osmotic water permeability per square centimeter of apical or basolateral cell membrane would be the same.

Morphometric measurements of the apical and basolateral surface areas of the *Amphiuma* early distal tubule indicate that the surface area of the basolateral cell membrane is ~13 times greater than the surface area of the apical cell membrane (Stanton et al., 1984). These results are similar to those made for the rabbit thick ascending limb (Welling and Welling, 1978). In both segments, the apical cell membrane lacks extensive surface area amplification. It is therefore possible that the asymmetry in the water permeability of the *Amphiuma* early distal tubule cell could be the result of differences in the surface areas of the two cells membranes and the relatively low water permeability of the apical cell membrane, a consequence of the absence of surface amplification. The results from this study indicate, however, that these differences in surface area cannot quantitatively account for the differences in hydraulic permeability.

We calculated the $L_p$ of the cell membranes per square centimeter of membrane (Table III) and found that the $L_p$ of the basolateral cell membrane is 2.5 times greater than the $L_p$ of the apical cell membrane. Since the hydraulic permeability of a cell depends upon both the intrinsic $L_p$ of the membranes and the surface area, it follows that the $L_p$ of the basolateral cell membrane per length of tubule is at least 33 times greater than that of the apical cell membrane. This is consistent with our observation (Table III) that reducing the osmolality of the luminal solution by 150 mosmol causes the cells to swell at a rate ~10 times lower than a 50-mosmol reduction of basolateral osmolality does. Thus, a low intrinsic water permeability and a relative lack of surface area amplification combine to make the apical cell membrane an effective barrier to water flow.

In studies on lumen collapsed mammalian proximal tubules, recent estimates of the $L_p$ of the basolateral cell membrane using video-optical techniques (Gonzalez et al., 1982; Welling et al., 1983) are in the range of $2\text{–}6 \times 10^{-4}$ cm·s$^{-1}$·osmol$^{-1}$ (calculated per centimeter of basolateral membrane area). Interestingly, these values are similar to those reported by Persson and Spring (1982) for the basolateral cell membrane of the *Necturus* gallbladder ($6.3 \times 10^{-4}$ cm·s$^{-1}$·osmol$^{-1}$). In comparison, the $L_p$ of the basolateral cell membrane of the early distal tubule is ~100 times smaller than the reported values for both the

mammalian proximal tubule and the *Necturus* gallbladder, which indicates that the basolateral cell membrane is also a significant barrier to transepithelial water flow. The relatively low water permeability of the *Amphiuma* early distal tubule is consistent with its role in the kidney as a barrier to water flow.

A possible source of error involved in our measurements of hydraulic water permeability is the presence of a significant unstirred layer. The influence of an unstirred layer on the measurement of $L_p$ has been reviewed in detail by House (1974). In general, if an unstirred layer next to an epithelium is relatively thick, and if the $L_p$ of the membrane is large, measurements of $L_p$ will yield an underestimate of the true value.

Many attempts have been made to correct for the influence of unstirred layers on the measurements of $L_p$ (see House, 1974, for a review). Most recently, Persson and Spring (1982) observed that the measured $L_p$ of the apical cell membrane of the *Necturus* gallbladder varied with the magnitude of the imposed osmotic gradient and they attributed this variation to the effect of an unstirred layer. By applying various osmotic gradients, they determined the $L_p$ of the apical cell membrane to be $2.5 \pm 0.3 \times 10^{-4}$ cm·s$^{-1}$·osmol$^{-1}$, with a hypo-osmotic gradient of 36 mosmol. Using a plot of $L_p$ vs. osmotic gradient and extrapolating to zero osmotic gradient, they estimated an $L_p$ uninfluenced by unstirred layer effects, assuming the unstirred layer effect could be minimized at very small osmotic gradients. Their corrected value for the $L_p$ of the apical cell membrane is $10 \times 10^{-4}$ cm·s$^{-1}$·osmol$^{-1}$, or four times greater than their measured value.

Similar experiments in the mammalian proximal tubule have yielded a quantitatively smaller influence of the magnitude of the imposed osmotic gradient on the measured $L_p$. For example, Gonzalez et al. (1982), using osmotic concentration differences from 44 to 11 mosmol, found only a twofold difference in the $L_p$ measured at 44 mosmol and the value obtained from an extrapolation to 0 mosmol. In similar experiments, Welling et al. (1983) observed no difference in the $L_p$ of $S_2$ segments of the rabbit proximal tubule measured at a hypotonic $\Delta C$ of 91.9–33.8 mosmol. Surprisingly, despite the very large $L_p$ values of these segments, it is clear that the influence of unstirred layers on the measurement of $L_p$ in mammalian renal tubules is not large.

A possible consequence of the existence of the unstirred layers in our preparation is that during the reduction in external osmolality, the composition of the solution at the outer surface of the cell membrane may not be the same as that of the bulk solution. The magnitude of this discrepancy can be estimated from the following equation (House, 1974):

$$\frac{C_m^o}{C_b^o} = \exp(J_v \delta^o / D), \tag{8}$$

where $C_m^o$ and $C_b^o$ are the solute concentrations at the outer surface of the membrane and in the bulk solution (Table I), respectively, $\delta^o$ is the thickness of the unstirred layer, $J_v$ is the volume flow (Table III), and $D$ is the diffusion coefficient for raffinose ($0.434 \times 10^{-5}$ cm$^2$·s$^{-1}$). If we assume that the thickness of the unstirred layer is 100 $\mu$m, the ratio calculated from Eq. 8 for the basolateral cell membrane is 1.03, which corresponds to an error in using $C_b^o$ to estimate $C_m^o$

of ~3%. Since the influence of unstirred layers on the measurement of apical cell membrane $L_p$ is even smaller than the basolateral cell membrane, it is clear that the unstirred layer effect is not a significant factor in our measurement of $L_p$ in the early distal tubule cells.

*Osmotic Swelling*

Early distal tubule cells of *Amphiuma* swell in response to a specific reduction of basolateral osmolality and do not exhibit any tendency to return to control volume. The magnitude of the osmotic response corresponds to the value predicted from the change in osmolality. A reduction in intracellular Cl activity, without a significant change in intracellular Cl content, is associated with cell swelling. The absence of a change in intracellular Cl content during swelling is consistent with the observation that the cells do not regulate cell volume.

To regulate cell volume after a reduction in osmolality, the cells must lose solute by stimulating exit pathways or by inhibiting entry pathways until a new steady state volume is achieved, at which point influx must again balance efflux. This transient imbalance in the two flux pathways does not occur in early distal tubule cells unless the cells are swollen after furosemide is perfused in the lumen. In the latter condition, the cells swell after a 50-mosmol reduction in basolateral osmolality but attain a volume that is smaller than predicted by the change in osmolality. This suggests that solute is lost from furosemide-treated cells, which is confirmed by our observation that osmotic swelling causes the intracellular Cl content to fall only after furosemide application. Thus, early distal tubule cells do contain transport systems that can affect net solute loss in response to an increase in volume, but only after the apical cotransport pathway is blocked. Additional support for this view comes from our observation that blocking the luminal cotransport system with furosemide causes a decrease in volume only in cells exposed to hypo-osmotic solutions (see Table VI). In this condition, furosemide induces a loss of anion from the cell at a flux, $3.3 \times 10^{-10}$ $M \cdot s^{-1} \cdot cm^{-2}$, that is comparable to the net reabsorptive flux of Cl by the tubule in control solutions. Thus, we speculate that in the absence of furosemide, transport systems that are moving solute out of the cell are stimulated by a decrease in bath osmolality; however, a net loss of solute does not occur, because of a matched stimulation of solute influx through the apical Na/K/Cl cotransporter.

A similar type of osmotically induced solute influx and efflux is known to occur in the frog skin epithelium (Ussing, 1982). For example, when the osmolality of the basolateral solution is lowered, frog skin cells swell and then partially adjust their volume back to control. This partial adjustment is associated with a loss of intracellular K. K loss can be doubled if furosemide is applied to the tissue before swelling. Ussing (1982) has proposed that osmotic swelling induces two transport systems. First, it increases Cl and K permeabilities to effect net K and Cl loss; second, it stimulates a cotransport system, which results in solute entry into the cells from the basolateral solution. Hence, analogous to the osmotic response of early distal tubule cells, the frog skin loses more solute when the entry pathway is blocked by furosemide.

Our observations suggest a difference between the regulation of volume in

response to changes in osmolality and to variations in net solute transport. To return volume to control after hypo-osmotic treatment, a cell must reduce the intracellular ion content by stimulating solute exit. On the other hand, to regulate cell volume in response to changes in net transport at constant extracellular osmolality, a cell must keep the intracellular ion content relatively constant. The apical and basolateral Cl-transporting systems of the early distal tubule do not operate separately to control cell volume in response to a reduction in osmolality, but are probably tightly coupled to maintain intracellular ion content and volume during changes in net solute transport at constant osmolality in response to variations in renal function. The importance of controlling, in concert, the movements of ions through apical and basolateral transport systems has been stressed recently in a review by Schultz (1982).

*Ouabain-induced Cell Swelling*

Inhibition of the basolateral Na/K pump by ouabain causes cell swelling and a depolarization of the basolateral cell membrane potential. Hence, it appears that although the early distal tubule cells do not regulate volume in response to a pure hypo-osmotic stimulus, they maintain their volume under normal transporting conditions by the action of the basolateral Na-K pump. The mechanism of action of ouabain is presumed to be an inhibition of basolateral Na/K ATPase, which limits the exit of Na from the cell. The continued entry of Na and Cl into the cell down a favorable gradient results in cell swelling. Ericson and Spring (1982*a*) and Larson and Spring (1983) recently confirmed this hypothesis by showing in the *Necturus* gallbladder that ouabain-induced cell swelling did not occur after maneuvers that inhibited apical Na/Cl entry. Similarly, our results indicate that inhibiting apical Na/K/Cl in the early distal tubule cells with furosemide limits ouabain-induced cell swelling and, in addition, diminishes the ouabain-associated depolarization of the basolateral cell membrane potential. Our data strongly suggest that the luminal Na/K/Cl cotransport system is a major pathway for ions to enter the cell.

In a transporting early distal cell, the basolateral Na/K pump plays a major role in moving Na out of the cell, while other transport pathways are responsible for the efflux of Cl and K. These other pathways for Cl and K probably derive their energy ultimately from the Na pump. Ouabain application inhibits the exit of Na from the cell through the Na/K pump but probably leaves some of the other transport mechanisms for ions to leave the cell functioning for some time. Thus, after ouabain treatment, cell swelling results from continued solute entry in the presence of lagging solute loss. Assuming that ouabain-induced swelling is the result of solute entry through the apical Na/K/Cl cotransport pathway and that Cl is the anion that enters the cell, a flux of Cl ( $J_{Cl}$) can be calculated using the initial rate of change in volume immediately after ouabain addition. $J_{Cl}$ calculated in this manner is $5.5 \times 10^{-11}$ $M \cdot cm^{-2} \cdot s^{-1}$ (based on luminal surface area). This accumulation of Cl in the cell is eight times smaller than the transepithelial net flux of Cl, which is an estimate of the rate of Cl movement through the cell (Oberleithner et al., 1982*a*). Thus, the net flux of Cl calculated from the rate of ouabain swelling cannot be attributed to a particular transport

system but represents the imbalance between Cl movement through the apical cotransporter and through basolateral transport systems.

We conclude from these studies (*a*) that the apical cell membrane acts both as a major site for ion transport and as a significant barrier to water flow, two characteristics that allow the early distal tubule to function as a diluting segment, and (*b*) that although the cells do not regulate volume in hypotonic media, they do maintain their volume under transporting conditions via a tight coupling of apical and basolateral transport systems.

## APPENDIX A*

### *Calculation of the Cellular Volume*

Longitudinal sections of cells like the ones indicated by the arrow in Figs. 1 and 2 can be described as containing all points $(x, y)$ such that

$$0 \leq x \leq L \quad \text{and} \quad 0 \leq y \leq f(x),$$

where

$$f(x) = h_o + \frac{4}{L^2}(h_m - h_o)(x)(L - x), \tag{A1}$$

and $h_o$ and $h_m$ are the minimum and maximum values of the thickness $h(x)$. This function describes a parabola and was chosen because in its integrable form it can be shown to be a reasonable approximation of the true profile (see the Discussion). The area of a maximal profile, $A_s$, is then given by

$$A_s = \int_o^L f(x) = L(\tfrac{1}{3}h_o + \tfrac{2}{3}h_m). \tag{A2}$$

If this section represents the average cellular profile around the circumference of the tubule, the volume of the cells for a length $L$ of tubule can be calculated as follows:

$$V = \pi \int_o^L \{[R_o]^2 - [R_i(x)]^2\}dx, \tag{A3}$$

where $R_o$ and $R_i$ are the outer and the inner radii, respectively. $R_o$ is constant, while $R_i(x)$ varies with $x$ in the following manner:

$$R_i(x) = R_o - f(x). \tag{A4}$$

Substituting Eq. A4 into A3 and rearranging gives

$$V = \pi \int_o^L [2R_o f(x) - f(x)^2]dx. \tag{A5}$$

Integrating Eq. A5,

$$V = \pi L\{[(R_o)^2 - (R_i)^2] + \tfrac{4}{3}R_i(h_m - h_o) - \tfrac{8}{15}(h_m - h_o)^2\} \tag{A6}$$

with $R_i = R_o - h_o$.

Eq. A6 gives a good approximation to the volume if the values of $h_o$ and $h_m$ represent averages around the circumference of the tubule. At any value of $x$, the values of $h(x)$

* The appendices were written by L. Mario Amzel.

vary around the circumference in a manner similar to that described for the axial dependence. Using the angular variable $\theta$ to describe the variations of $h(x)$ and assuming that there are $n$ maxima $h_m(x)$ and minima $h_o(x)$ around the circumference, the behavior of $h(x)$ for $0 \leq \theta \leq 2\pi/n$ is

$$h(x, \theta) = h_o(x) + [h_m(x) - h_o(x)] \frac{n^2}{\pi^2}\left(\frac{2\pi}{n} - \theta\right)\theta. \tag{A7}$$

To simplify the final equations, $h(x, \theta)$ can be replaced by an average value $\overline{h(x)}$, which, for example, gives the correct area for the sections of all cells around the tubule at $x$. Remembering that the area of revolution can be obtained as

$$A_c = \tfrac{1}{2}\int_o^{2\pi} R^2 d\theta, \tag{A8}$$

the area of the cellular sections is

$$A_s(x) = \frac{n}{2}\int_o^{2\pi/n} \{(R_o)^2 - [R_o - h(x, \theta)]^2\} d\theta. \tag{A9}$$

Integrating Eq. A9,

$$A_s(x) = \pi(R_o)^2 - \pi\{[R_o - h_o(x)]^2 - \tfrac{4}{3}[R_o - h_o(x)][h_m(x) - h_o(x)] + \tfrac{8}{15}[h_m(x) - h_o(x)]^2\}. \tag{A10}$$

If the average $\overline{h(x)}$ is used, the second term in Eq. A10 should be equal to

$$\begin{aligned}\pi[R_o - \overline{h(x)}]^2 &= \pi\{[R_o - h_o(x)] - [\overline{h(x)} - h_o(x)]\}^2 \\ &= \pi\{[R_o - h_o(x)]^2 - 2[R_o - h_o(x)][\overline{h(x)} - h_o(x)] + [\overline{h(x)} - h_o(x)]^2\}.\end{aligned} \tag{A11}$$

For Eqs. A10 and A11 to be approximately equal,

$$2[\overline{h(x)} - h_o(x)] \approx \tfrac{4}{3}[h_m(x) - h_o(x)] \tag{A12}$$

and

$$[\overline{h(x)} - h_o(x)] \approx 0.73[h_m(x) - h_o(x)]. \tag{A13}$$

Eqs. A12 and A13 can be averaged to give a single equation:

$$\overline{h(x)} - h_o(x) = 0.7[h_m(x) - h_o(x)] \tag{A14}$$

or

$$h(x) = 0.7h_m(x) + 0.3h_o(x). \tag{A15}$$

Using Eq. A15, one can obtain

$$h_o = 0.7h_m(0) + 0.3h_o(0) \tag{A16}$$

and

$$h_m = 0.7h_m(L/2) + 0.3h_o(L/2). \tag{A17}$$

The values of $h_o$ and $h_m$ obtained using Eqs. A16 and A17 and the experimental values for $h_m(0)$, $h_o(0)$, $h_m(L/2)$, and $h_o(L/2)$ can be used in Eq. A6 to give a good approximation of the volume.

If the maximum and minimum $h$ along the axial direction and along the circumference

are the same, the formula for the volume obtained by the double integration (integration in $x$ and $\theta$) is quite compact:

$$V = \frac{n}{2}\int_o^L \int_o^{2\pi/n} (R_o)^2 \left[(R_i)^2 - \frac{4\pi^2}{L^2 n^2}(h_m - h_o)(x)(L - x)(\theta)\left(\frac{2\pi}{n} - \theta\right)\right]^2 dx d\theta; \quad \text{(A18)}$$

$$V = \pi l[(R_o)^2 - (R_i)^2 - 8/9(h_m - h_o)R_i - (8/15)^2(h_m - h_o)^2]. \quad \text{(A19)}$$

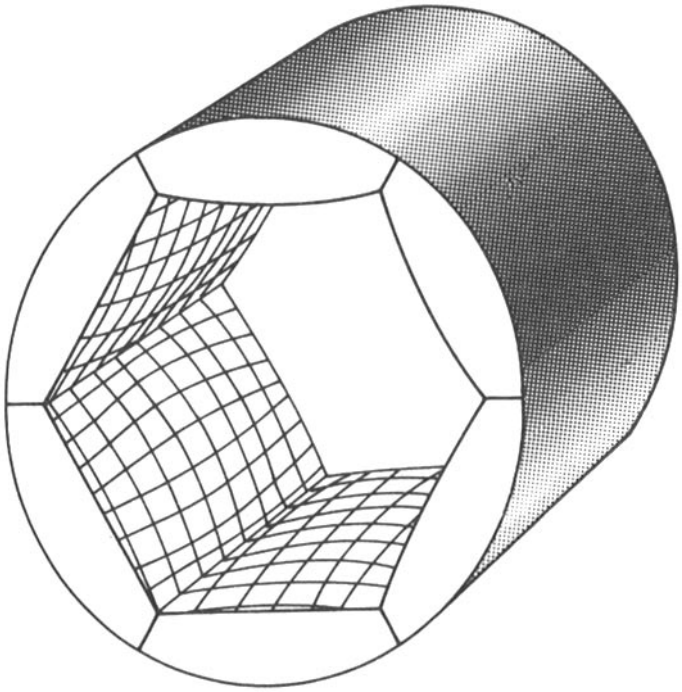

FIGURE 8. A computer-generated model of the tubule determined from the approach outlined in Appendix A. It should be pointed out, first, that although this figure depicts six cells in the annulus, our equations are independent of the number of cells, and, second, that the figure does not represent an average profile of cells along a renal tubule. It does show that our model projects the profile of one cell around the annulus of a tubule.

Using arguments similar to those involved in the derivation of Eqs. A16 and A17,

$$V \approx L[(R_o)^2 - (R_o - \langle h \rangle)^2] \quad \text{(A20)}$$

with

$$\langle h \rangle \approx 0.49 h_m + 0.51 h_o, \quad \text{(A21)}$$

where 0.49 was obtained as the average of 8/15 and 8/18.

The representation of a tubule segment represented by these equations with $N = 6$ is shown in Fig. 8.

## APPENDIX B

### *Calculation of Cellular Volume from Serial Sections*

If $m$ sections are measured, each separated by a distance $\delta$ (centimeters) and having area $A_i$ (square centimeters), the volume is

$$V_m = \delta \sum_{i=1}^{m} A_i. \tag{B1}$$

This volume can be used to estimate the cellular volume around the complete circumference by realizing that

$$\frac{V_m}{V} = \frac{A_m}{A}, \tag{B2}$$

where $A_m$ is the shaded area in Fig. 9 and $A$ is the complete area of the circular corona.

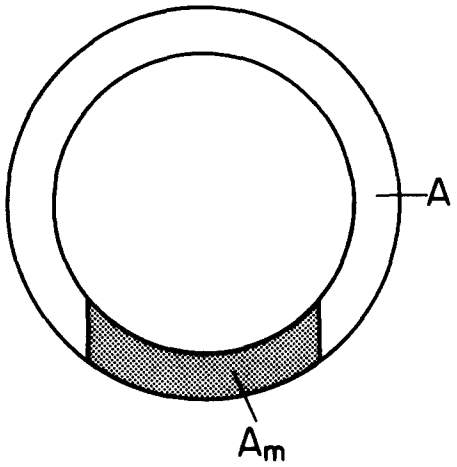


FIGURE 9. Surface area of the tubule optically sectioned ($A_s$) and the remaining surface area ($A$).

In the figure, the length of the shaded area is $m\delta$.

$$A_m = 2\int_o^{d/2} [(R_o)^2 - x^2]^{1/2} dx - 2\int_o^{d/2} [(R_i)^2 - x^2]^{1/2} dx. \tag{B3}$$

Integrating Eq. B3,

$$A_m = \frac{d}{2}\left[(R_o)^2 - \frac{d^2}{4}\right]^{1/2} + (R_o)^2 \arcsin\left(\frac{d}{2R_o}\right) - \frac{d}{2}\left[(R_i)^2 - \frac{d^2}{4}\right]^{1/2} - (R_i)^2 \arcsin\left(\frac{d}{2R_i}\right) \tag{B4}$$

for $R_i \geq d/2$. The area $A$ is simply

$$A = \pi[(R_o)^2 - (R_i)^2] \tag{B5}$$

and $V$ can be evaluated as

$$V = (V_m)(A/A_m). \tag{B6}$$

Special thanks go to Dr. Ken Spring for his advice in the setup of our video-optical system and for his comments on the manuscript. We also thank Dr. Guillermo Whittembury for his helpful discussions on unstirred layer effects.
This work was supported by grants AM-32061 to W.B.G. and AM-17433 to G.G. from the National Institute of Arthritis, Diabetes, and Digestive and Kidney Diseases.

*Original version received 15 November 1983 and accepted version received 21 March 1985.*

## REFERENCES

Baumgarten, C. M. 1982. An improved liquid ion exchanger for chloride ion-sensitive microelectrodes. *Am. J. Physiol.* 241:C258–C263.

Burg, M., J. Grantham, M. Abramow, and J. Orloff. 1966. Preparation and study of fragments of single rabbit nephrons. *Am. J. Physiol.* 210:1293–1298.

Cala, P. M. 1980. Volume regulation by *Amphiuma* red blood cells. The membrane potential and implications regarding the nature of ion-flux pathways. *J. Gen. Physiol.* 76:683–708.

Carpi-Medina, P., E. Gonzalez, and B. Whittembury. 1983. Cell osmotic water permeability of isolated rabbit proximal convoluted tubules. *Am. J. Physiol.* 244:F554–F563.

Davis, C. W., and A. L. Finn. 1981. Regulation of cell volume of frog urinary bladder. *In* Membrane Biophysics: Structure and Function in Epithelia. Alan R. Liss, Inc., New York. 25–36.

Ericson, A. C., and K. R. Spring. 1982*a*. Coupled NaCl entry into *Necturus* gallbladder epithelial cells. *Am. J. Physiol.* 243:C140–C145.

Ericson, A. C., and K. R. Spring. 1982*b*. Volume regulation by *Necturus* gallbladder: apical $Na^+$-$H^+$ and $Cl^-$ $HCO_3^-$ exchange. *Am. J. Physiol.* 243:C146–C150.

Fujimoto, M., and T. Kubota. 1976. Physiochemical properties of a liquid ion exchanger microelectrode and its application to biological fluids. *Jpn. J. Physiol.* 26:631–650.

Gagnon, J., D. Ouimet, H. Nguyen, R. Laprade, C. Le Grimellec, S. Carriere, and J. Cardinal. 1982. Cell volume regulation in the proximal tubule. *Am. J. Physiol.* 243:F408–F415.

Ganote, C., J. J. Grantham, H. L. Moses, M. B. Burg, and J. Orloff. 1968. Ultrastructural studies of vasopressin effect on isolated perfused renal collecting tubules of the rabbit. *J. Cell Biol.* 36:355–367.

Gonzalez, E., P. Carpi-Medina, and G. Whittembury. 1982. Cell osmotic water permeability of isolated rabbit proximal straight tubules. *Am. J. Physiol.* 242:F321–F330.

Greger, R. 1981. Chloride reabsorption in the rabbit cortical thick ascending limb of the loop of Henle. A sodium dependent process. *Pflügers Arch. Eur. J. Physiol.* 390:38–43.

Greger, R., and E. Schlatter. 1981. Presence of luminal $K^+$, a prerequisite for active NaCl transport in the cortical thick ascending limb of Henle's loop of rabbit kidney. *Pflügers Arch. Eur. J. Physiol.* 392:92–94.

Guggino, W. B., B. A. Stanton, and G. Giebisch. 1982. Electrical properties of isolated distal tubule of *Amphiuma*. *Fed. Proc.* 14:1579. (Abstr.)

House, C. R. 1974. Water Transport in Cells and Tissues. Edward Arnold London. 562 pp.

Katz, A. I. 1982. Renal Na-K ATPase: its role in tubular sodium and potassium transport. *Am. J. Physiol.* 242:F207–F219.

Kirk, K. L., J. A. Schafer, and D. R. DiBona. 1984. Microscopic methods for analysis of function in isolated renal tubules. *In* Membrane Biophysics. II. Physical Methods in the Study of Epithelia. Alan R. Liss, Inc., New York. 21–36.

Kleinzeller, A., and A. Knotkova. 1964. The effect of ouabain on electrolyte and water transport in kidney cortex and liver slices. *J. Physiol. (Lond.)*. 175:172–192.

Larson, M., and K. R. Spring. 1983. Bumetanide inhibition of NaCl transport by *Necturus* gallbladder. *J. Membr. Biol.* 44:123–129.

Leaf, A. 1956. On the mechanism of fluid exchange of tissues *in vitro*. *Biochem. J.* 62:241–248.

Linshaw, M. A. 1980. Effects of metabolic inhibitors on renal tubule cell volume. *Am. J. Physiol.* 239:F571–F577.

Linshaw, M. A., and F. B. Stapleton. 1978. Effect of ouabain and colloid osmotic pressure on renal tubule cell volume. *Am. J. Physiol.* 235:F480–F491.

MacRobbie, E. A. C., and H. H. Ussing. 1961. Osmotic behavior of the epithelial cells of frog skin. *Acta Physiol. Scand.* 53:348–365.

Oberleithner, H., W. B. Guggino, and G. Giebisch. 1982*a*. Mechanism of distal tubular chloride transport in *Amphiuma* kidney. *Am. J. Physiol.* 242:F331–F339.

Oberleithner, H., F. Lang, W. Wang, and G. Giebisch. 1982*b*. Effects of inhibition of chloride transport on intracellular sodium activity in distal amphibian nephron. *Pflügers Arch. Eur. J. Physiol.* 394:55–60.

Oberleithner, H., R. Greger, F. Neuman, F. Lang, G. Giebisch, and P. Deetjen. 1983*a*. Omission of luminal potassium reduces cellular chloride in early distal tubule of *Amphiuma* kidney. *Pflügers Arch. Eur. J. Physiol.* 398:18–22.

Oberleithner, H., W. Guggino, G. Giebisch. 1983*b*. The effect of furosemide on luminal sodium, chloride, and potassium transport in the early distal tubule of the *Amphiuma* kidney. *Pflügers Arch. Eur. J. Physiol.* 396:27–33.

Oberleithner, H., F. Lang, R. Greger, W. Wang, and G. Giebisch. 1983*c*. Effect of luminal potassium on cellular sodium activity in the early distal tubule of *Amphiuma* kidney. *Pflügers Arch. Eur. J. Physiol.* 396:34–40.

Oberleithner, H., M. Ritter, F. Lang, and W. Guggino. 1983*d*. Anthracene-9-carboxylic acid inhibits renal chloride reabsorption. *Pflügers Arch. Eur. J. Physiol.* 398:172–174.

Persson, B., and K. R. Spring. 1982. Gallbladder epithelial cell hydraulic water permeability and volume regulation. *J. Gen. Physiol.* 79:481–505.

Schultz, S. G. 1982. Homocellular regulatory mechanisms in sodium-transporting epithelia: avoidance of extinction by "flush through." *Am. J. Physiol.* 241:577–590.

Spring, K. R., and A. Hope. 1979. Fluid transport and the dimensions of cells and interspaces of living *Necturus* gallbladder. *J. Gen. Physiol.* 73:287–305.

Stanton, B., D. Biemesderfer, D. Stetson, M. Kashgarian, and G. Giebisch. 1984. Cellular ultrastructure of *Amphiuma* distal nephron: effects of exposure to potassium. *Am. J. Physiol.* 247:C204–C216.

Stoner, L. C. 1977. Isolated, perfused amphibian renal tubules: the diluting segment. *Am. J. Physiol.* 233:F438–F444.

Ussing, H. H. 1982. Volume regulation of frog skin epithelium. *Acta Physiol. Scand.* 114:363–369.

Weinman, S. A., and L. Reuss. 1984. $Na^+$-$H^+$ exchange and $Na^+$ entry across the apical membrane of *Necturus* gallbladder. *J. Gen. Physiol.* 83:57–74.

Welling, L. W., and D. J. Welling. 1978. Shape of cells and intercellular channels in rabbit thick ascending limb of Henle. *Kidney Int.* 13:144–151.

Welling, L. W., D. J. Welling, and T. J. Ochs. 1983. Video measurement of basolateral membrane hydraulic conductivity in the proximal tubule. *Am. J. Physiol.* 245:F119–F122.